Environ. Sci. Technol. **1999**, *33,* 553−559

Aerosol and Product Yields from NO_3 Radical-Initiated Oxidation of Selected Monoterpenes

MATTIAS HALLQUIST,*,† INGVAR WÄNGBERG,‡ EVERT LJUNGSTRÖM,† IAN BARNES,§ AND KARL-HEINZ BECKER§

Department of Inorganic Chemistry, University of Göteborg, SE - 412 96 Göteborg, Sweden, Swedish Environmental Research Institute, P.O. Box 47086, SE - 402 58 Göteborg, Sweden, and Institut für Physikalische Chemie/FB 9, Bergische Universität Gesamthochschule Wuppertal, Gaussstrasse 20, D-42097 Wuppertal, Germany

Atmospheric transformation of monoterpenes gives products that may cause environmental consequences. In this work the NO_3 radical-initiated oxidation of the monoterpenes α-pinene, β-pinene, Δ^3-carene, and limonene has been investigated. All experiments were conducted in EUPHORE, the EUropean PHOto REactor facility in Valencia, Spain. The aerosol and product yields were measured in experiments with a conversion of the terpenes in the interval from 7 to 400 ppb. The lower end of the concentrations used are close to those measured in ambient pine forest air. Products were measured using long path in situ FTIR. Aerosol yields were obtained using a DMA-CPC system. The aerosol mass yields measured at low concentrations (10 ppb terpene reacted) were <1, 10, 15, and 17% for α-pinene, β-pinene, Δ^3-carene, and limonene, respectively. The total molar alkylnitrate yields were calculated to be 19, 61, 66, and 48%, and molar carbonyl compound yields were estimated to be 71, 14, 29, and 69% for α-pinene, β-pinene, Δ^3-carene, and limonene, respectively. The aerosol yields were strongly dependent on the amounts of terpene reacted, whereas the nitrate and carbonyl yields do not depend on the amount of terpene converted. The principal carbonyl compound from α-pinene oxidation was pinonaldehyde. In the case of limonene, endolim was tentatively identified and appears to be a major product. The reactions with β-pinene and Δ^3-carene yielded 1−2% of nopinone and 2−3% caronaldehyde, respectively. The results show that it is not possible to use generalized descriptions of terpene chemistry, e.g. in matematical models.

Introduction

A recent estimate of emissions of biogenic hydrocarbons to the atmosphere has highlighted monoterpenes as an important class of compounds with a yearly estimated global emission of 127 Tg carbon (*1*). Such high emissions warrant investigations of the atmospheric chemistry of these compounds. The knowledge obtained until now is scarce but is well summarized by Atkinson (*2*). One reason for the lack of information may be experimental problems, caused by formation of oxidation products giving aerosol particles, thus requiring additional analytical tools for identification and quantification of the condensed phase. The high concentrations often used for smog chamber studies enhance the aerosol particle formation (*3*). However, the formation of aerosol particles also occurs in the ambient atmosphere at significantly lower concentration of the reactants (*4*, *5*). Aerosol particle formation is of great concern for air quality since particles affect visibility and can be troublesome from an human health aspect (*6*). Further, the organic aerosol formation may produce nuclei that eventually could serve as cloud condensation nuclei (CCN) and thereby have an impact on cloud formation (*7*). A change in CCN concentration could alter the global albedo and as a consequence also affect the climate (*8*, *9*).

Oxidation of unsaturated hydrocarbons, e.g. terpenes, in the atmosphere is initialized by ozone, hydroxyl radicals, or by nitrate radicals. The dominant process is determined by the individual rates of reaction which, in turn, are dependent on the concentration of the oxidants. Generally, OH radicals are most important during day time and NO_3 radicals during night time. The ozone concentration is not purely dependent on photochemistry, and therefore this oxidant has to be considered for both night- and daytime conditions.

The oxidation of terpenes initiated by the NO_3 radical is known to also produce nitrated species (*2*, *10*−*12*). These compounds can act as a temporary reservoirs of odd nitrogen in the atmosphere. Depending on their lifetimes, nitrated compounds could transport nitrogen oxides over considerable distances (*13*, *14*).

Here we report results from an aerosol and gas-phase product study of the reactions between the NO_3 radical and α-pinene, β-pinene, Δ^3-carene, and limonene. The concentration of terpenes was varied between 400 and 10 ppb. The lower end of this range corresponds to concentrations found in Scandinavian pine forest air during summer night time (*15*).

Experimental Section

All experiments were performed in one of the two large reactors at the EUropean PHOto REactor facility (EUPHORE) in Valencia. This facility has two half-spherical Teflon bags, each with a volume of about 200 m^3 and has been described previously (*16*, *17*). The reactors are shielded by two retractable half-spherical protective housings which, when closed, also exclude sunlight from the reactors, thereby allowing dark chemistry experiments to be carried out during the day. To achieve homogeneous concentrations, two mixing fans are placed inside each chamber. All experiments were made at 1002−1015 mbar using purified dry air as the bath gas. The air purification system was capable of maintaining the inlet air particle concentration between 50 and 100 cm^{-3}. The size distribution of this aerosol was flat but centered well below 0.1 μm. The ice point was typically −47° C (corresponding to a relative humidity of 0.5% at 284 K, the lowest temperature for any experiment). Figure 1 shows the structures of the investigated compounds together with some oxygenated products. Table 1 presents a summary of the experimental conditions.

The products were observed using long path FTIR spectroscopy and some also by sampling on DNPH (2,4-dinitrophenylhydrazine) coated C_{18}-cartridges for HPLC analysis. The infrared system consists of a NICOLET MAGNA

* Corresponding author phone: +44 1223 336362; fax: +44 1223 336519; e-mail: hallq@inoc.chalmers.se.
† University of Göteborg.
‡ Swedish Environmental Research Institute.
§ Bergische Universität Gesamthochschule Wuppertal.

10.1021/es980292s CCC: $18.00
Published on Web 01/05/1999

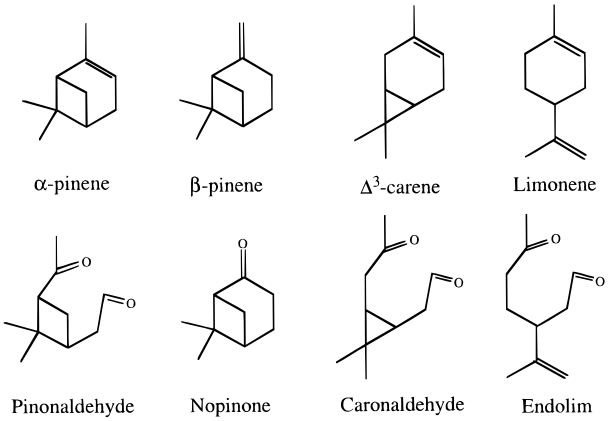

FIGURE 1. Structures of the investigated terpenes and of some of the expected carbonyl products.

TABLE 1. Experimental Conditions[a]

terpene	temp (°C)	initial concns (ppb) [N_2O_5]	initial concns (ppb) [terpene]	initial particle concn (cm^{-3})
α-pinene	18	387	580	26
α-pinene	20	278	420	not available
α-pinene	15	99	140	6200
α-pinene	12	9.1	18	35
α-pinene	17	8.9	18	15
β-pinene	13	358	580	95
β-pinene	11	95	140	650
β-pinene	20	39	72	100
β-pinene	16	7.0	18	31
Δ^3-carene	11	395	580	40
Δ^3-carene	21	96	140	50
Δ^3-carene	16	97	140	150
Δ^3-carene	16	97	140	93
Δ^3-carene	20	6.8	18	46
limonene	13	10.2	18	38

[a] The initial concentrations of particles were recorded after the introduction of N_2O_5.

TABLE 2. Absorption Cross Sections Used in This Study[a]

compound	wavenumber (cm^{-1})	absorption cross section (cm^2 molecule^{-1}) (base 10)	ref
NO_2	1602	$(4.71 \pm 0.26) \times 10^{-19}$	17
N_2O_5	1246	8.56×10^{-19}	17
alkylnitrates	800−900	$(1.46 \pm 0.09) \times 10^{-17}$ [a]	12
pinonaldehyde	1725	$(3.51 \pm 0.14) \times 10^{-19}$	18
caronaldehyde	1742	$(4.52 \pm 0.22) \times 10^{-19}$	18
nopinone	1743	$(5.43 \pm 1.08) \times 10^{-19}$	this study

[a] Average integrated absorption cross section (cm molecule^{-1}).

550 FTIR spectrometer, operated at 1.0 cm^{-1} spectral resolution and equipped with an MCT-detector. The instrument is connected to a White mirror system with a base path length of 8.17 m. The optical path length employed was 326.8 m. Spectra were recorded by co-adding between 36 and 115 scans. This resulted in a time resolution of between 1 and 3.2 min. The evaluation was done using reference spectra to subtract NO_2, N_2O_5, HNO_3, and the terpene before analyzing the product features. Quantification was done using the absorption cross sections presented in Table 2 at the stated wavenumbers.

DNPH-cartridge sampling for HPLC analysis was used in one Δ^3-carene and one β-pinene experiment. This provided a complimentary method for quantitative detection of carbonyl compounds, e.g. caronaldehyde and nopinone. The type of cartridge used was C_{18}, coated with DNPH. The sampling was performed at the end of the experiments by drawing chamber air through the cartridges with an air flow of 1.1 L min^{-1}. The samples were eluted with acetonitrile, allowed to react for 1 min, and then injected on a 1050 series Hewlett-Packard HPLC equipped with a diode array UV-detector. The identification and quantification of the carbonyls were performed using authentic reference samples. The sampling method was checked in the β-pinene experiment by adding 10 ppb of nopinone to the chamber after the first sampling. A second sample showed a 90% recovery of nopinone.

The number-size distributions of the aerosol formed in the reactions between NO_3 radicals and the terpenes were studied by using a TSI 3071 Differential Mobility Analyzer (DMA). The DMA was equipped with an inlet impactor with a 50% cutoff at 0.51 μm and connected to a TSI 3022 Condensation Particle Counter (CPC) serving as the detector. The number concentrations were measured in 17 intervals and interpolated to obtain data in 32 intervals, covering the size range between 0.012 and 0.535 μm. Data were corrected for the fraction of charged particles, multiply charged particles, DMA transmission function, and CPC efficiency to give actual number concentrations. Particle volume concentrations were calculated assuming the particles to be spheres. Particles in each interval were counted, after an appropriate stabilization period, for 30 s or until 3000 particles were detected. The total time for measurement of a size distribution was typically 10−15 min. The instruments were installed just below the reaction chamber floor and connected to the chamber by a 50 cm long, 0.4 cm i.d. stainless steel tube protruding 15 cm above the chamber floor. A second CPC was also connected to this sampling probe. The latter instrument registered the total particle concentration. When both CPC instruments were connected directly to the probe, they showed identical readings over a wide concentration span. Number loss rate coefficients, including both coagulation and wall deposition, were typically $(3-7) \times 10^{-5}$ s^{-1}.

All experiments were initiated by first introducing N_2O_5 to the reactor. The method and equipment for preparing and introducing N_2O_5 has been descibed earlier, and only a short decription will be given here (*17*). Prior to introduction, N_2O_5 was prepared in a flow reactor where O_3 was mixed with excess NO_2. The flows of NO_2 in nitrogen and O_3 in oxygen and their contact-time were adjusted so that no O_3 was left in the mixture when introduced into the chamber. With this set-up the reactor could be charged with 15 ppb of N_2O_5 per minute. When the desired concentration of N_2O_5 was achieved, the terpene was introduced by evaporating it into a stream of air entering just below one of the two mixing fans.

Between experiments, the reactor was cleaned by flushing with purified air. It was, however, noted that aerosols sometimes were formed during introduction of N_2O_5. Events with nucleation of 10^4 cm^{-3} were sometimes encountered. One plausible explanation is that reactive impurities from earlier experiments were not fully removed by flushing. No trace of any candidate impurity could be seen with the FTIR system. The problem was solved by adding sufficient N_2O_5 to remove any reactive compound after each experiment.

At the beginning of an experiment, the chamber has a homogeneous concentration of NO_2, N_2O_5, and NO_3. Even if it was possible to mix the terpene instantaneously into the reactor, the reaction rate would be such that even the slowest reacting substance, β-pinene, would deplete the available supply of nitrate radicals in a few seconds. In reality it is expected that terpene concentrations, at least during the introduction, will be higher close to the inlet despite the action of the mixing fans. After this short initial stage, the reaction rate would be controlled by the decomposition of

TABLE 3. Yield of Products and Aerosol Particulate Matter from Reaction of NO_3 with Monoterpenes[d]

α-Pinene

N_2O_5 reacted (ppb)	$\Delta[N_2O_5]/\Delta$[terpene]	nitrate yield (%)	NO_2 loss (%)	estimated total yield of carbonyls (%)	yields of pinonaldehyde (%)	aerosol yield (%)
387	0.93	21	22	70	65	[0.2][a]
278	–	19	17	68	64	16[b]
99	–	25	20	76	71	7
9.1	–	18	17	75	71	0.3
8.9	–	20	15	76	72	0.7

β-Pinene

N_2O_5 reacted (ppb)	$\Delta[N_2O_5]/\Delta$[terpene]	nitrate yield (%)	NO_2 loss (%)	estimated total yield of carbonyls (%)	yields of nopinone (%)	aerosol yield (%)
358	1.01	66	86	14	–	[13][a]
95	0.94	68	85	12	–	[39][a]
39	1.02	74	57	14	1–2	52
7.0	–	61	59	–	–	10

Δ^3-Carene

N_2O_5 reacted (ppb)	$\Delta[N_2O_5]/\Delta$[terpene]	nitrate yield (%)	NO_2 loss (%)	estimated total yield of carbonyls (%)	yield of caronaldehyde (%)	aerosol yield (%)
395	1.01	69	82	23	–	62
96	–	74	71	29	–	55
97	–	68	74	24	2–3	56
97	–	–	–	–	–	49
6.8	–	66	66	29	–	15

Limonene

N_2O_5 reacted (ppb)	$\Delta[N_2O_5]/\Delta$[terpene]	nitrate yield (%)	NO_2 loss (%)	estimated total yield of carbonyls (%)	estimated yield of endolim (%)	aerosol yield (%)
10.2	–	48	40	69	69	17

[a] Number-size distribution partly outside the measured range. [b] Aerosol yield measured by A. Virkkula using a similar DMA-CPC system (20). [c] (–) not available. [d] The aerosol yields are expressed in mass percent. All other yields were calculated on a molar basis. See text for definition of table entries.

N_2O_5, and the rate of product formation would not differ much between the different terpenes. In all experiments, the terpene was added in excess thus restricting secondary reactions between the products and NO_3.

Chemicals. Chemicals used were (1*S*)-(−)-α-pinene > 97% Merck, (1*S*)-(−)-β-pinene 99% Aldrich, (+)-Δ^3-carene > 93% TCI, (*R*)-(+)-limonene > 97% Merck, and (1*R*)-(+)-nopinone 98%, Aldrich. Pinonaldehyde and caronaldehyde were synthesized by ozonolysis of the corresponding terpene (*18*, *19*).

Results

Product Analysis. All experiments in which the relation: consumed N_2O_5 versus reacted terpene could be measured, i.e., those with high initial concentrations, show a ratio close to 1:1. For β-pinene this ratio could also be measured at lower concentrations as is shown in Table 3. Since the N_2O_5 consumed ($\Delta[N_2O_5]$) could always be measured, all estimates of yield are calculated assuming a 1:1 relation between the N_2O_5 and terpene consumed. This 1:1 ratio was also observed earlier by Wängberg *et al.* (*12*), who determined an $\Delta[N_2O_5]/\Delta$[α-pinene] ratio of 1.01 ± 0.07.

A product analysis has been made by comparing the features in the end product spectra from β-pinene, Δ^3-carene, and limonene with product spectra from α-pinene for which most of the products have been identified and the yields determined (*11*, *12*). This comparison makes possible identification of the principal product categories, i.e., alkylnitrates and carbonyl compounds. Product spectra from α-pinene, β-pinene, and Δ^3-carene are presented in Figure 2. The position of the previously identified peaks for products from α-pinene oxidation are indicated (*12*). Absorptions from alkylnitrates are clearly recognizable also for Δ^3-carene and

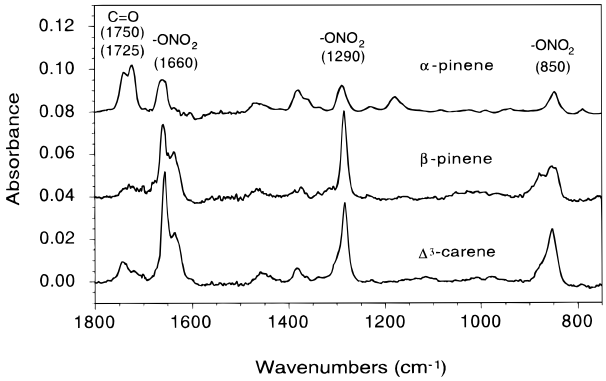

FIGURE 2. Spectra corresponding to products from conversion of 100 ppb α-pinene, β-pinene, and Δ^3-carene. Absorptions due to NO_2, terpene, and HNO_3 have been subtracted. The alkylnitrate bands appear at 850, 1290, and 1660 cm^{-1}. Carbonyl features are seen between 1720 and 1760 cm^{-1}.

β-pinene. The quantification of the alkylnitrates is based on the integrated band absorption at 800–900 cm^{-1} using an average integrated cross section of 2-hydroxypinane-3-nitrate and 3-oxopinane-2-nitrate (*12*). Estimated yields of carbonyls in the case of β-pinene were calculated assuming that the carbonyl absorption cross sections were identical to that of nopinone and in the case of Δ^3-carene and limonene to that of caronaldehyde. In the α-pinene experiments, pinonaldehyde was both identified and quantified by FTIR–subtraction using calibrated reference spectra. The estimate of total yield of carbonyl compounds for α-pinene does, in addition to pinonaldehyde, include the yield of 3-oxopinan-2-nitrate that was calculated using the 21% fraction of nitrate

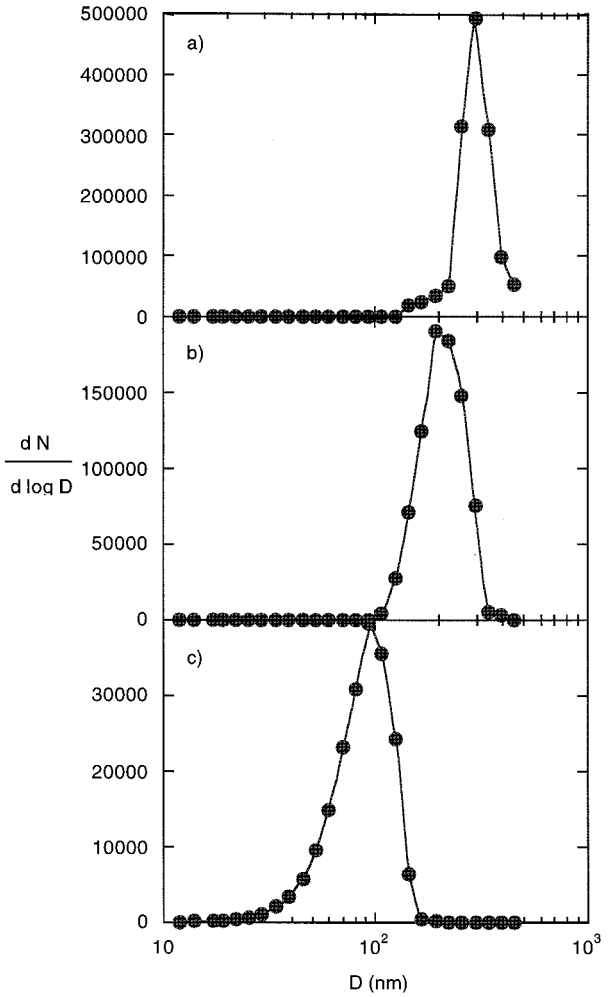

FIGURE 3. Aerosol particle number distribution measured in Δ^3-carene experiments: (a) 395 ppb reacted, (b) 96 ppb reacted, and (c) 6.8 ppb reacted.

yield determined in an earlier study (*12*). The result is shown in Table 3 where the yields for alkylnitrates and carbonyl compounds are given on a molar basis.

NO_2 loss is defined as

$$\frac{[NO_y](\text{start}) - [NO_y](\text{end})}{\Delta[N_2O_5]} \quad \text{where}$$

$$[NO_y] = [NO_2] + 2[N_2O_5] \quad \text{(I)}$$

and constitutes an alternative method of estimating the yield of nitrogen containing compounds, i.e., alkylnitrates. The nitrate yields obtained from the integrated nitrate band area and from the NO_y mass-balance agree well for α-pinene, thus indicating that the NO_2 loss is due to formation of alkylnitrate compounds. The nitrate yields estimated from integrated nitrate band areas, for β-pinene and Δ^3-carene, are somewhat lower than those estimated from NO_2 loss in experiments made at high concentrations but agree well for experiments with lower start concentrations. The agreement between the two independent estimates lends some confidence to the presented nitrate yields.

Aerosol Measurements. The chemical reaction occurs on a time scale much shorter than that of the aerosol measurements. What is observed is essentially the final result, and no further development of the aerosol due to chemical causes can be seen. Figure 3 shows, as an example, the number-size distributions recorded for Δ^3-carene after the chemical oxidation and mixing processes have ceased.

TABLE 4. Aerosol Particle Number Concentrations

terpene	N_2O_5 reacted (ppb)	total no. concn (cm^{-3})	D_{max} (nm)	d *N*/d log *D* (D_{max} interval)
α-pinene	387	[150][a]	453	720
α-pinene	278	–	–	–
α-pinene	99	14 000	143, 255[b]	77 000, 28 000
α-pinene	9.1	40	60, 191[b]	3, 150
α-pinene	8.9	30	93, 191, 453[b]	57, 52, 91
β-pinene	358	[610][a]	523	2800
β-pinene	95	[6000][a]	392	28 000
β-pinene	39	10 000	255	36 000
β-pinene	7.0	710	221	2100
Δ^3-carene	395	88 000	294	490 000
Δ^3-carene	96	230 000	124	740 000
Δ^3-carene	97	53 000	191	190 000
Δ^3-carene	97	68 000	165	224 000
Δ^3-carene	6.8	12 000	93	39 000
limonene	10.2	9600	124	19 000

[a] Number-size distribution partly outside the measured range. [b] Distribution has multiple maxima. [c] (–) not available. [d] D_{max} is the mean diameter in the interval that contains the maximum number concentration. d *N*/d log *D* is the distribution peak value.

Table 4 presents the total number of concentrations and position of the distribution maxima of all experiments. Table 3 gives the calculated aerosol yields obtained from the number-size distributions. The mass of particles present before the addition of terpene but after the addition of N_2O_5 was calculated from number-size distributions measured before terpene addition. The mass of these particles was in most cases negligible compared to the mass formed in the reactions. However, in cases where very little new aerosol mass was formed, i.e., the low and medium concentration α-pinene experiments, the observed mass after the experiments was corrected by subtracting the initial mass. The greatest correction was made for the 140 ppb α-pinene experiment (cf. Table 1) and amounted to 3 percentage units. The yields are expressed as mass percent of reacted terpene, assuming a product density of 1.0 g cm^{-3}. Since the molecular weight of the products is likely to be higher than that of the terpene, the mass yield is an upper limit of the corresponding molar yield. In most of the experiments the size distributions fall well within the measuring range of the equipment. However, in some cases the distribution falls, to an unknown extent, above the available range and the measured yield is too low. In Tables 3 and 4, the experiments for which the distribution falls partly outside the measured ranges are marked and the values must not be used, e.g. for calculating mass balances.

Discussion

Although the terpenes studied have similar chemical structure, the results presented in Tables 3 and 4 indicate that they react to give quite different product distributions. Hence, the yields of carbonyls and nitrates as well as the ability to form aerosols varies significantly among the studied terpenes. As one may expect, the yields of condensed matter are strongly dependent on the amount terpene reacted (*3*, *21*). As may be seen from Table 3, β-pinene, Δ^3-carene, and limonene, in contrast to α-pinene, all gave significant aerosol yields even when small amounts are oxidized.

The chemical composition of the particulate matter could not be analyzed in this study, but the presence of absorption bands in the infrared spectra recorded in experiments with high concentrations gives an indication about the nature of particle constituents. In a recent study (*12*), it was found that the position of the strong nitrate infrared absorption band near 1660 cm^{-1} is lowered by approximately 30 cm^{-1} in the

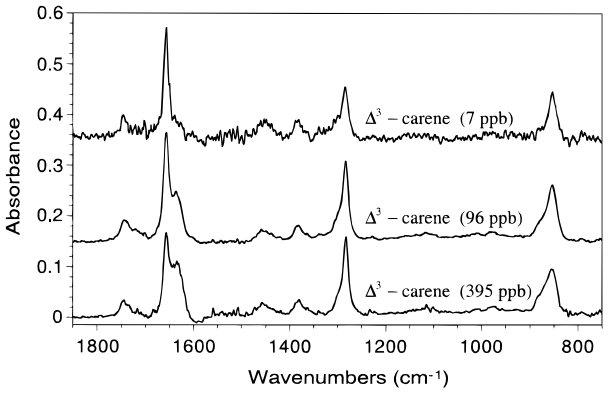

FIGURE 4. Product spectra from Δ^3-carene showing the concentration dependence of nitrate absorptions in the condensed phase at 1630 cm^{-1}. The spectrum corresponding to 395 ppb Δ^3-carene reacted is shown in its original scale. The two spectra measured for 96 and 7 ppb Δ^3-carene reacted are scaled by multiplying the *y*-axis values with 395/96 and 395/7, respectively. Absorptions due to NO_2, HNO_3, and Δ^3-carene have been subtracted.

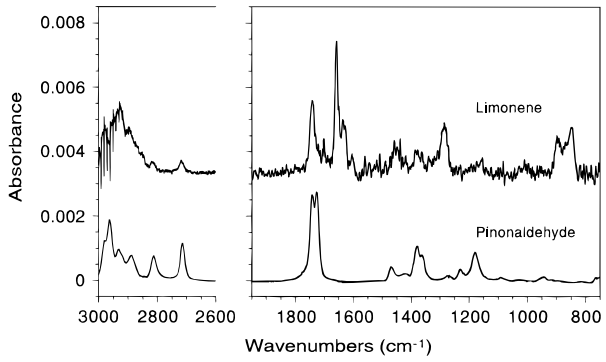

FIGURE 5. Product spectrum measured in the limonene experiment. A reference spectrum of pinonaldehyde is shown for comparison of carbonyl and aldehydic hydrogen band frequencies. The reference spectrum has been scaled to represent approximately 10 ppb of pinonaldehyde.

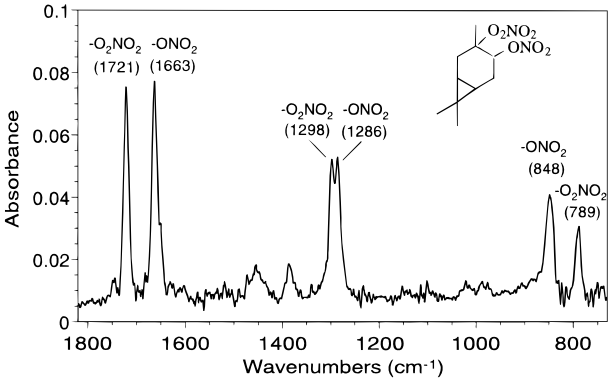

FIGURE 6. FTIR spectrum of products formed in an initial stage of NO_3 radical reaction with Δ^3-carene in a high concentration experiment. Absorptions from NO_2, N_2O_5, HNO_3, and Δ^3-carene have been subtracted. Wavenumbers corresponding to the center of $-ONO_2$ and $-O_2NO_2$ absorptions are indicated in the figure.

liquid-phase compared to the gas-phase. Because of the presence of a second band at lower wavenumbers in the product spectra from the NO_3-α-pinene reaction it was suggested that the additional band was due to absorption by condensed matter produced in the reactions. The additional absorption only occurred in spectra from experiments in which high amounts of α-pinene were oxidized, i.e., experiments yielding aerosols. The appearance of the same spectral features and their assignment to aerosol formation was further verified in this work. Concerning *β*-pinene and Δ^3-carene, nitrate double peaks also appear in experiments where small amounts of terpenes were oxidized as is shown in Figure 2. With the lowest start concentrations of *β*-pinene and Δ^3-carene, however, no double peaks could be seen. This is shown in Figure 4 using the example with Δ^3-carene. When further comparing the product yields given in Table 3, it appears that *β*-pinene and Δ^3-carene form much more nitrates than does α-pinene. On the other hand, the present result also shows that the formation of carbonyl compounds from *β*-pinene and Δ^3-carene is less than in the α-pinene case. The yields of alkylnitrate, carbonyl compound, and aerosols, presented in Table 3, are in general not additive since carbonyl and alkylnitrate groups may occur in the same molecule, e.g. 3-oxopinane-2-nitrate found by Wängberg *et al.* (*12*) in the oxidation of α-pinene. Also, the obtained yield for alkylnitrates and carbonyls could include molecules that are present in the condensed phase as mentioned before. The yields of alkylnitrates and carbonyl compounds from α-pinene, *β*-pinene, and Δ^3-carene appear, within the accuracy of the measurements, to be independent of their initial concentrations. Hence, a similar alkylnitrate and carbonyl product distribution can be expected under ambient atmospheric conditions.

Pinonaldehyde is the principal product in the reaction of NO_3 with α-pinene and the yields obtained here are in good agreement with previous work (*11*, *12*). Pinonaldehyde is also a product in the reactions between α-pinene and OH radicals as well as from ozone initiated oxidation (*2*, *22*−*26*). Ozone and OH reaction with *β*-pinene and Δ^3-carene are reported to yield significant amounts of nopinone and caronaldehyde, respectively (*2*, *22*−*27*). A comparison was made between authentic spectra of nopinone and caronaldehyde and the product spectra from experiments with *β*-pinene and Δ^3-carene. Neither of these carbonyls could be detected in the corresponding product spectra. However, low concentrations of nopinone and caronaldehyde were detected using DNPH−cartridge sampling for HPLC analysis. In the *β*-pinene−NO_3 experiment 1−2% nopinone was detected, and from the Δ^3-carene oxidation 2−3% of caronaldehyde was found. The product spectra were also examined for aldehydic hydrogen stretching absorption in the region 2650−2820 cm^{-1}, but no traces of aldehyde bands could be detected. This is also in agreement with the HPLC analysis since caronaldehyde has relatively strong aldehydic hydrogen bands (*18*, *26*) and since formaldehyde would also be formed together with nopinone (*2*, *22*, *24*, *27*). Thus, no significant formation of the expected products, nopinone and caronaldehyde, occurred at the conditions applied in this work.

Concerning limonene, for which only one experiment was made, the yield of both nitrates and carbonyls are high as is shown in Figure 5 and Table 3. The limonene reaction also yielded more aerosols than α-pinene. However, as for α-pinene, more carbonyls than nitrates are formed. Aldehydic stretching absorptions at 2716 and 2815 cm^{-1} in addition to the strong carbonyl band at 1740 cm^{-1} shows that a keto-aldehyde similar to pinonaldehyde is produced. This strongly suggest that the NO_3 radical attack takes place on the ring double bond with bond rupture resulting in formation of endolim. A keto-aldehyde compound with the same absorption band positions has been reported to be formed in OH initiated reactions of limonene by Hakola *et al.* (*26*) and was tentatively identified as endolim by these authors.

Infrared absorptions due to nitroperoxy groups were seen in spectra recorded during an early phase of the oxidations of all terpenes before end-products dominated the spectra. One example, Δ^3-carene, is given in Figure 6, and the absorptions are attributed to a nitroperoxy-alkylnitrate

compound formed via addition of NO_3 to one of the carbon atoms in the double bond, most likely the least substituted carbon (*28*), to form an alkylnitrate radical which then adds an O_2 molecule to form a peroxy radical. The peroxyradical, in turn, may undergo reactions with other peroxy radicals or react with NO_2 according to reaction 1 to form the nitroperoxy-alkylnitrate compound.

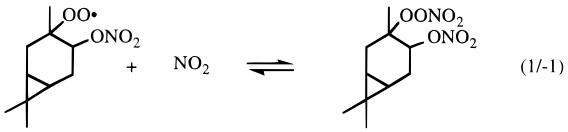

(1/-1)

The observed peroxynitrate compounds disappeared very quickly, showing that they are quite unstable and are likely to decompose according to reaction −1. The appearance of nitroperoxy-alkylnitrate compounds has been reported in several other NO_3−alkene product studies (*2*, *11*, *12*). The observation of such compounds here indicates that the initial step of the oxidation mechanism is similar to other structurally less complex alkenes.

One relevant question is why the investigated terpenes give final aerosols that differ with respect to number concentration and size distribution to the extent shown in Table 4. This issue has been addressed by Wang *et al.* (*29*), who used a comprehensive mathematical model containing gas phase production of the condensable species, nucleation of the same, and coagulation and growth by condensation to simulate the temporal development of an aerosol. They successfully applied the model to interpret secondary aerosol data obtained in a smog chamber experiment. Key parameters, influencing particle number concentration and size distribution, were found to be the formation rate of condensable product, the product molecular weight, its gas−liquid equilibrium pressure, the product surface tension, and the total amount of condensable matter produced.

The reaction rate in all our experiments is controlled by the rate of N_2O_5-decomposition and does not depend on the specific terpene oxidized. The product formation rate can therefore be ruled out as a cause for the observed differences between the terpenes. However, this rate may influence the results obtained at different N_2O_5 start concentrations.

For low vapor pressures of the initially nucleating substance, a change by a factor of 100 caused changes in peak number concentration and volume mean diameter by factors of 330 and 5, respectively (*29*). A high equilibrium vapor pressure gives rise to fewer and larger particles than does a lower pressure. The equilibrium pressures of the nucleating products in our experiments are difficult to estimate, and only an upper boundary could be set. If 10 ppb of terpene is consumed, if 15% (cf. aerosol yields in Table 3) is turned into the nucleating compound and if a supersaturation ratio of 10 is needed to induce significant nucleation, then it follows that the equilibrium pressure has to be lower than 0.015 Pa (0.15 ppb). Compounds with an equilibrium pressure exceeding this limit would not induce nucleation although at a later stage they may dissolve in already existing particles to some extent (*3*). This rules out C_{10} dicarbonyls such as caronaldehyde and pinonaldehyde as the nucleating species (*18*), while dicarboxylic acids, substituted monocarboxylic acids, and other strongly polar disubstituted compounds are likely candidates. The results from this study deliver evidence for the tendency of nitrate species to occur in the condensed phase, and it is therefore likely that at least one of the substituents on the condensing species is an $-ONO_2$ group. Even though Wang's experiment (*29*) took place on a much longer time scale than the present experiments, it is clear that the observed differences in size distributions may well be caused byproducts having different vapor pressures.

The multimodal behavior of the size distribution that was observed for some experiments is believed to be caused by the initial presence of aerosol particles in the reactor. Product condensation on existing particles takes place in parallel with nucleation of new particles. Not even the presence of comparatively high initial concentrations of particles, e.g. in the 99 ppb α-pinene experiment, is sufficient to suppress nucleation and two strong modes result.

The surface tension of the products is very important since the nucleation rate has an exponential, third power dependence on this parameter (*29*). The final appearance of a size distribution is at least as sensitive to this quantity as to the equilibrium partial pressure. The lack of information about nucleating products from the reactions studied in this work excludes further speculation about the influence of surface tension and molecular weight.

To more closely investigate the dynamics of the aerosol formation from terpene−nitrate radical reactions, we are at present performing modeling studies of these systems.

Atmospheric Implications. The difference in behavior between the different monoterpenes is clearly noticeable, both with respect to the distribution between the gaseous and condensed phase and between the type of products observed. This shows that it is not in general possible to lump terpene reactions in work with mathematical models, covering the atmospheric chemistry of terpenes, if any confidence is to be had concerning the impact of these terpenes on the result. The high yield of gaseous first-generation products, e.g. pinonaldehyde from α-pinene, indicates that there is a potential for further reactions, possibly contributing to tropospheric oxidant formation.

The nitrate radical reactions either rapidly cycle nitrogen back to nitrogen dioxide when carbonyl compounds are formed or may give reasonably stable alkylnitrates that act as temporary reservoirs of NO_x. These nitrates could serve as a means of transporting nitrogen oxides over considerable distances until photolysis reactivates the odd nitrogen.

Aerosol formation is of some importance since particulates may serve as condensation nuclei for other low-vapor pressure compounds and eventually contribute to the CCN concentration. Indications of aerosol formation have been reported in studies of NO_3 reactions with terpenes (*10*, *21*). However, this is, to our knowledge, the first time that aerosol yields from NO_3−terpene reactions have been quantified. The results show that it is reasonable to expect aerosol formation even at ambient concentrations of the reactants for many monoterpenes. Thus oxidation of terpenes, initiated by NO_3 radicals, constitutes a night time source of aerosol particles.

Acknowledgments

This work was supported financially through the EU Environment and Climate BIOVOC project ENV4 CT95 0059. The experimental work was carried out in the EUPHORE smog chamber facility at the Fundación CEAM, Valencia, Spain. The authors acknowledge the interest and financial support by the Generalidad Valenciana and Fundacióne BANCAIXA. We are also indebted to Millán M. Millán and Klaus Wirtz, CEAM, Valencia, Spain, for their assistance and technical support in the use of the EUPHORE chamber. Thanks are due to Manuel Pons for conducting the HPLC analysis and to Aki Virkkula for providing additional aerosol yield data. I.W. thanks the European Commission for a Human Resources and Mobility grant.

Literature Cited

(1) Guenther, A.; Hewitt, C. H.; Erickson, D.; Fall, R.; Geron, C.; Graedel, T.; Harley, P.; Klinger, L.; Lerdau, M.; McKay, W. A.;

Pierce, T.; Scholes, B.; Steinbrecher, R.; Tallamraju, R.; Taylor, J.; Zimmerman, P. *J. Geophys. Res.* **1995**, *100*, 8873.
(2) Atkinson, R. *J. Phys. Chem. Ref. Data* **1997**, *26*(2), 215.
(3) Odum, J. R.; Hoffmann, T.; Bowman, F.; Collins, D.; Flagan, R. C.; Seinfeld, J. H. *Environ. Sci. Technol.* **1995**, *30*, 2580.
(4) Went, F. W. *Nature* **1960**, *187*, 641.
(5) Marti, J. J.; Weber, R. J.; McMurry, P. H.; Eisele, F.; Tanner, D.; Jefferson, A. *J. Geophys. Res.* **1997**, *102*(D5), 6331.
(6) Donaldson, K.; Li, X. Y.; MacNee, W. *J. Aerosol Sci.* **1998**, *29*, 553
(7) Novakov, T.; Penner J. E. *Nature* **1993**, *365*, 823.
(8) Twomey, S. A.; Piepgrass, M.; Wolfe T. L. *Tellus* **1984**, *36B*, 356
(9) Charlson, R. J.; Schwartz, S. E.; Hales, J. M.; Cess, R. D.; Coakley, J. A., Jr; Hansen, J. E.; Hofmann, D. J. *Science* **1992**, *255*, 423
(10) Barnes, I.; Bastian, V.; Becker, K. H.; Tong, Z. *J. Phys. Chem.* **1990**, *94*, 2413.
(11) Berndt, T.; Böge, O. *J. Chem. Soc., Faraday Trans.* **1997**, *93*, 3021.
(12) Wängberg, I.; Barnes, I.; Becker, K. H. *Environ. Sci. Technol.* **1997**, *31*, 2130.
(13) Talukdar, K. R.; Herndon, S. C.; Burkholder, J. B.; Roberts, J. M.; Ravishankara, A. R. *J. Chem. Soc., Faraday Trans.* **1997**, *93*(16), 2787.
(14) Talukdar, K. R.; Burkholder, J. B.; Hunter, M.; Gilles, M. K.; Roberts, J. M.; Ravishankara, A. R. *J. Chem. Soc., Faraday Trans.* **1997**, *93*(16), 2797.
(15) Janson R. *J. Atmos. Chem.* **1993**, *14*, 387.
(16) Becker, K. H. Final Report of the EC-Project "The European Photoreactor EUPHORE" Contract EV5V-CT92-0059, 1995.
(17) Wängberg, I.; Etzkorn, T.; Barnes, I.; Platt, U.; Becker, K. H. *J. Phys. Chem. A* **1997**, *101*, 9694.
(18) Hallquist, M.; Wängberg, I.; Ljungström E. *Environ. Sci. Technol.* **1997**, *31*, 3166.
(19) McMurry, J. E.; Bosch, J. *Org. Chem.* **1987**, *52*, 4885.
(20) Virkkula, A. Manuscript in preparation.
(21) Hoffmann, T.; Odum, J. R.; Bowman, F.; Collins, D.; Klockow, D.; Flagan, R. C.; Seinfeld, J. H. *J. Atmos. Chem.* **1997**, *26*, 189.
(22) Hatakeyama, S.; Izumi, K.; Fukuyama, T.; Akimoto, H. *J. Geophys Res.* **1989**, *94*, 13013.
(23) Arey, J.; Atkinson, R.; Aschmann, S. M. *J. Geophys Res.* **1990**, *95*, 18539.
(24) Hatakeyama, S.; Izumi, K.; Fukuyama, T.; Akimoto, H.; Washida, N. *J. Geophys Res.* **1991**, *96*, 947.
(25) Grosjean, D.; Williams, E. L., II.; Seinfeld, J. H. *Environ. Sci. Technol.* **1992**, *26*, 1526.
(26) Hakola, H.; Arey, J.; Aschmann, S. M.; Atkinson R. *J. Atmos. Chem.* **1994**, *18*, 75.
(27) Grosjean, D.; Williams, E. L., II.; Grosjean, E.; Andino, J. M.; Seinfeld, J. H. *Environ. Sci. Technol.* **1993**, *27*, 2754.
(28) Wayne, R. P.; Barnes, I.; Biggs, P.; Burrows, J. P.; Canosa-Mas, C. E.; Hjorth, J., LeBras, G.; Moortgat, G. K.; Perner, D.; Poulet, G.; Restelli, G.; Sidebottom, H. *Atmos. Environ.* **1991**, *25A*, 1−203.
(29) Wang, S. C.; Flagan, R. C.; Seinfeld, J. H. *Atmos. Environ.* **1992**, *26A*, 421.

Received for review March 25, 1998. Revised manuscript received October 5, 1998. Accepted October 29, 1998.

ES980292S